Received: 10 July 2017 | Revised: 20 August 2018 | Accepted: 11 October 2018

DOI: 10.1002/eco.2053

RESEARCH ARTICLE

WILEY

Hydrologic responses to climate warming for a snow-dominated watershed and a transient snow watershed in the California Sierra

Kyongho Son[1,2,3] | Christina Tague[3]

[1] Research Foundation of the City University of New York, New York City, New York

[2] Hunter College, City University of New York, New York

[3] Bren School of Environmental Science and Management, University of California, Santa Barbara, California

Correspondence
Kyongho Son, Research Foundation of the City University of New York, New York City, NY.
Email: kson@dep.nyc.gov

Funding information
National Science Foundation, Grant/Award Number: EAR-0725097

Abstract

Climate warming will have substantial impacts on hydrological fluxes in the California Sierra. A commonly used approach for assessing these impacts, particularly in mountain watersheds, is to substitute space for time. This conceptual model assumes that with warming, the hydrologic behaviour of higher elevation snow dominated watersheds (SDWs) will converge to the hydrologic behaviour of lower elevation transient snow watersheds (TSWs). To investigate the efficacy of this conceptual model, a process-based model (RHESSys) was applied to a TSW and a SDW with a mean annual temperature 2 °C lower than the TSW in the Sierra National forest, California. This study investigated the effect of climate warming (2 and 4 °C) on the model estimates of snow water equivalent (SWE), streamflow, evapotranspiration (ET), and moisture deficit in the two watersheds. Modelling results show that SDW under 2 °C warming scenarios generates monthly SWE similar in magnitude and timing as TSW under historic conditions. However, SDW under 2 °C warming scenarios generates higher annual and summer streamflow due to shallower groundwater storage and experiences less water limitation due to lower ET, compared with TSW under historical climate conditions. In both watersheds, leaf area index and wetness index are primary factors controlling spatial patterns of seasonal ET under both historical climate conditions and warming scenarios. Climate warming increases the spatial variability in monthly ET, especially in the summer period. These modelling results suggest that vegetation structure and subsurface properties may be as important as climate in explaining hydrologic response to climate warming in small Sierra Nevada watersheds.

KEYWORDS

California Sierra, climate warming, ecohydrology, geology, RHESSys, snow process, vegetation

1 | INTRODUCTION

Climate warming in the mountain regions of the Western United States has altered snow, soil moisture, vegetation water use, and streamflow. However, the magnitude and timing of these effects varies both between and within watersheds (Christensen, Tague, & Baron, 2008; Howat & Tulaczyk, 2005; Tague & Grant, 2009). Mountain watersheds have steep topographic gradients, and therefore, the spatial patterns of hydrologic variables (snow, soil moisture, and ET) may vary with climate change. Complex interactions among topography, soil, vegetation, and geology cause the hydrologic variables to respond differently to climate warming.

Geological difference is one of the key factors controlling the sensitivity of hydrologic responses to climate warming. Tague and Grant (2009) demonstrated that geologic differences and elevation gradients explain differences in streamflow response to climate

warming between watersheds in the High and Western Cascades, Oregon. Their modelling study showed that watersheds with slow draining, deep groundwater, such as those of the High Cascades in Western Oregon, have four times greater reduction of August streamflow under 1.5 °C warming scenarios than neighbouring fast draining watersheds dominated by Western Cascade geology. Similarly, Safeeq, Grant, Lewis, and Tague (2013) examined observed streamflow sensitivity to climate variability between watersheds in the Western United States. They similarly concluded that watersheds dominated by deep groundwater are more sensitive to climate warming than watersheds dominated by shallow groundwater.

Patterns of snow accumulation and melt are another factor that is likely to influence the sensitivity of hydrologic responses to warming. Assessments of the vulnerability of snow to temperature increases have identified locations with "snow at risk" as those where snow frequently falls near zero degrees (Klos, Link, & Abatzoglou, 2014; Nolin & Daly, 2006). However, there has been no consensus about whether streamflow from snow-dominated watersheds (SDWs) is more sensitive to climate warming relative to streamflow from watersheds with substantial snow at risk or transient snow watersheds (TSWs; Jefferson, 2011). Safeeq et al. (2013) demonstrated that climate warming reduces the ratio of summer flow to annual precipitation more in SDWs than in TSWs. However, Nolin and Daly (2006) showed that TSWs in the Pacific Northwest region are more sensitive to climate warming than the SDWs. Thus, although snow patterns may be more sensitive in TSWs, this may not translate into changes in patterns of other ecohydrologic variables (such as streamflow, soil moisture, and ET) and suggests that climate warming's effects on TSWs and SDWs may vary with other landscape properties, such as vegetation and geology (Peel & Bloschl, 2011). In this study, we assess whether these underlying landscape properties may confound simple relationships between a changing snowpack and other ecohydrologic variables and their spatial patterns.

Hydrologic models are used to predict changes in snow regime, vegetation water use, and streamflow for future climate conditions. Studies using hydrologic models have improved our understanding of how hydrologic processes may be altered under projected climate change (Jasper, Calanca, & Fuhrer, 2006; Tague & Grant, 2009). Process-based models include key hydrologic processes and potentially accounts for the feedback of these processes to climate change. This study uses the Regional Hydrologic-Ecologic Simulation System (RHESSys; Tague & Band, 2004), process-based, physical, hydrologic model to better understand difference in hydrologic response to climate warming between a TSW and a SDW. RHESSys couples hydrologic processes, carbon cycling processes, and soil geochemical cycling processes (nitrogen and carbon) into the model. RHESSys has been applied to study climate change impacts in many watersheds across North America (Hwang, Band, & Hales, 2009; Mackay, Samanta, Nemani, & Band, 2003; Tague & Peng, 2013), Europe (Zierl, Bugmann, & Tague, 2007), and Asia (Kim, Kang, & Lee, 2007), and the model successfully reproduced observed streamflow, evapotranspiration (ET), and carbon fluxes in these studies.

This study uses a process-based model approach to predict the effects of climate warming on two small Sierra Nevada watersheds (Figure 1): P303, a TSW and B203, a SDW. Specifically, this study investigates the impacts of climate warming on (a) seasonal and interannual variation of hydrologic fluxes in TSW and SDW and (b) the spatial structure of seasonal ET and its relationship with physiographic parameters in TSW and SDW. As well, this study tests whether the difference of climate parameters between TSW and SDW can explain the hydrologic responses to climate warming.

2 | METHODOLOGY

2.1 | Study sites

The two study sites, the Providence subwatershed (P303, 1.32 km^2) and the Bull subwatershed (B203, 1.4 km^2), are located in the King River Basin (Figure 2) and part of King River Experimental Watershed and Southern Sierra Critical Zone Observatory. P303 is classified as TSW, and B203 is classified as a SDW (Hunsaker, Whitaker, & Bales, 2012). In both watersheds, precipitation mostly occurs between October and April. Snow in SDW accumulates earlier, with higher peak accumulations, and melts later than in TSW. The difference in average daily temperature between the watersheds is about 2 °C, and annual precipitations are similar (Table 1). Each watershed has two climate stations (Upper and Lower Providence climate stations for TSW and Upper and Lower Bull climate stations for SDW): one located near or at the top and the other station located near the bottom of the watershed. The climate stations measure weather parameters (precipitation, air temperature, relative humidity, global solar radiation, wind speed and direction, snow depth, and snow water equivalent [SWE]) at 15-min interval. Each watershed has two streamflow gauge stations at the outlet to measure low and high flows.

The elevation of TSW ranges from 1,730 to 1,990 m, and the elevation of SDW ranges from 2,185 to 2,490 m (Figure 2; Table 1). TSW has steeper slopes than SDW with a slightly lower wetness index (Beven & Kirkby, 1979). The two watersheds are covered with Sierran mixed conifer forest with some mixed chaparral and barren land cover. Sierran mixed conifer is composed of white fir (*Abies concolor*), red fir (*Abies magnifica*), ponderosa pine (*Pinus ponderosa*), Jeffrey pine (*Pinus Jeffrey*), black oak (*Quercus kelloggii*), sugar pine (*Pinus lambertiana*), and incense cedar (*Calocedrus decurrens*). The dominant tree of TSW is white fir, but the dominant tree of SDW is red fir. The 10-m leaf area index (LAI) was derived from Light Detecting and Ranging point cloud using a deterministic approach (Richardson, Moskal, & Kim, 2009; Table 1). TSW has denser tree cover (and higher LAI) than SDW. The dominant soil type is Shaver (66%) in TSW and Cagwin (80%) in SDW. These two soil types are highly permeable and have high percentages of sand.

2.2 | RHESSys model

The RHESSys is a physically based spatially explicit model used to investigate effects of climate warming on hydrologic fluxes in TSW and SDW, two distinct Sierra Nevada watersheds. RHESSys is under continuous development, and in this study, version 5.15.r326 was used. A detailed description of the model equations is provided in Tague and Band (2004).

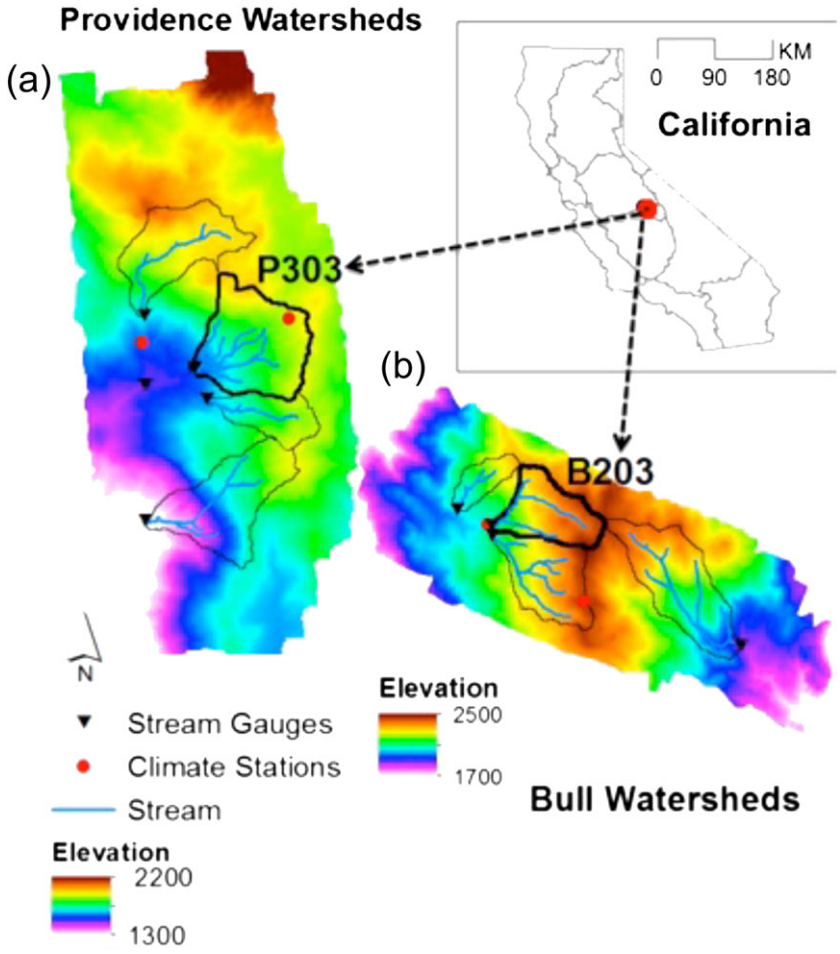

FIGURE 1 Study sites. (a) Providence watersheds and (b) Bull watersheds: (circle) climate stations and (triangle) streamflow stations. P303 is one of subwatersheds in Providence and is used to represent a transient snow watershed, and B3203 is one of subwatersheds in Bull and is used to represent a snow-dominated watershed

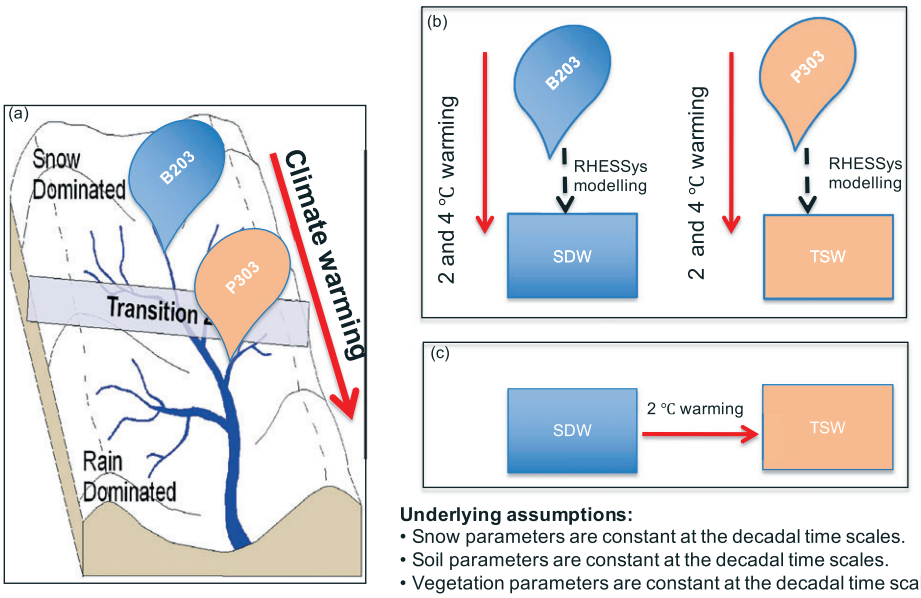

FIGURE 2 A framework for examining the effect of climate warming on hydrologic responses in the two small Sierra Nevada watersheds: (a) P303 is located in transient snow zone, and B203 is located in snow-dominated zone. (b) 2 and 4 °C warming scenarios are applied to the two watersheds and are compared with the two watersheds' hydrologic responses to the two warming scenarios, and (c) to isolate the effect of climate warming relative to other hydrologic properties (vegetation and geology), the transient snow watershed (TSW) under historical climate conditions is compared with the snow dominated watershed (SDW) under 2 °C warming

The key hydrological processes in the RHESSys model include snow accumulation and melt, soil infiltration, ET, and both shallow and deep groundwater flow. To calculate the snow accumulation rate, an estimation of the snowfall in the total precipitation is required. For periods when measurements of snowfall are available, snowfall data are used as an input. Otherwise, the partitioning of total precipitation

TABLE 1 Basic hydrologic properties of the P303 and the B203 (Hunsaker et al., 2012)

Watershed	P303 (TSW)	B203 (SDW)
Elevation	1,730 to 1,990 m	2,185 to 2,490 m
Aspect	SW	SW
Slope	1.3 to 30.3 (12.73)	0.9 to 24.9(11.38)
Vegetation	Mixed Sierra conifer (Dominant tree species: white fir) LAI distribution: 0 to 9.1 (2.6)	Mixed Sierra conifer (Dominant tree species: red fir) LAI distribution: 0 to 5.7 (1.2)
Soil	Dominant soil types: Shaver (66%) Strongly weathered quartz diorite Permeability: Moderately rapid Hydrologic soil group: B	Dominant Soil types: Cagwin (80%) Highly weathered granitic rock Permeability: Rapid Hydrologic soil group: A
Precipitation/Run-off	Precipitation type: Snow–rain transition Mean annual precipitation (2005 to 2007): 1,513 mm; run-off ratio (R/P): 0.20	Precipitation type: Snow-dominated Mean annual precipitation (2005 to 2007): 1,517 mm; run-off ratio (R/P): 0.53
Temperature	Daily average temperature (°C) of 2004 to 2007 (mean ± *SD*): Min: 4.5 ± 0.8 Max: 10 ± 1.0 Mean: 8.6 ± 0.9	Daily average temperature (°C) of 2004 to 2007 (mean ± *SD*): Min: 3 ± 1.1 Max: 11.2 ± −0.7 Mean: 6.8 ± 0.8
Drainage pattern	Wetness index: 4.1 to 13.8 (7.2)	Wetness index: 4.1 to 15.9 (7.2)

Note. LAI: leaf area index; SD: standard deviation; SDW: snow dominated watershed; TSW: transient snow watershed.

in rain and snow is estimated using daily average temperature. To account for the uncertainty of the temperature threshold value used to define the phase of precipitation, dual temperature threshold values are used (Marks, Winstral, Reba, Pomeroy, & Kumar, 2013). RHESSys uses a quasienergy balance snowmelt model. Snowmelt is computed using radiation-driven melt and melts due to the combination of sensible and latent heats, and advective heat-driven melt, occurring as rainfall on snow. The minimum climate data required for model simulation include daily precipitation and daily maximum and minimum air temperature data. Other climate data including solar radiation, saturation vapour pressure, relative humidity, and so on are computed using a climate interpolation model (MT-CLIM; Glassy & Running, 1994). RHESSys simulates vegetation ET based on Penman–Monteith equation (Monteith, 1965) with a stomatal physiology adapted from Jarvis (1976). Although potential evapotranspiration (PET) is not used directly by the model, it is calculated to support output analysis. In the PET, canopy conductivity for the Penman–Monteith estimate is calculated with maximum species-level stomata conductivity times estimated LAI values. Soil infiltration is based on Philip equation (Philip, 1957). The drainage rate of infiltrating water from the unsaturated zone to the saturated zone is computed based on field capacity and unsaturated hydraulic conductivity (Clapp & Hornberger, 1978). Preferential flow through soil macropores and bedrock fractures is computed by assuming that a fixed percentage of infiltrated water bypasses the soil zone and infiltrates to deep groundwater storage. Lateral shallow groundwater flow is calculated using transmissivity and local slope. Deep groundwater flow is calculated using a linear storage model.

Patches are the finest spatial model unit in RHESSys and is used to account for spatial variation in radiation, precipitation, and air temperature forcing conditions. The 10-m Light Detecting and Ranging digital elevation model (DEM) was used to derive the patch map. Each watershed was assigned "mixed conifer" as the vegetation type, as spatial information about vegetation species is not available. Associated vegetation parameters for the mixed conifer vegetation type were taken from RHESSys parameter libraries (https://github.com/RHESSys/ParamDB), and vegetation parameters are based on White, Thornton, Running, and Nemani (2000). A set of allometric equations were used to initialize carbon and nutrient stores in vegetation. The rooting depths for TSW and SDW were estimated based on Hunsaker et al. (2012): 2 m for TSW and 1 m for SDW. Soil properties were assumed to be spatially homogenous at watershed scale, as soil data are limited to parameterize soil properties at fine scales. Initial soil properties for each soil type are estimated based on existing RHESSys parameter libraries.

2.3 | Model calibration

This study used daily snow depth and SWE data and measured daily streamflow data to calibrate snow and soil parameters. The three snow parameters include (a) the lapse rates for the daily maximum and minimum air temperature, (b) temperature threshold values for the partition of snow and rain in the total precipitation and (c) an empirical temperature melt coefficient (accounting for snowmelt due to latent and sensible heat). Because the fine-spatial scale temperature is not available, air temperature values within the watersheds were estimated with elevation-based temperature lapse rates. Temperature threshold values and the empirical temperature melt coefficient were calibrated by comparing the SWE model estimates with the measured snow depth of the two climate stations for each watershed (or measured SWE in the Upper Providence station and the Upper Bull station). To compare the model estimate of SWE and measured snow depths, we calculated the day of complete snowmelt in the four climate stations. It was assumed that the snow-related parameters do not change with climate warming.

After estimating the snow-related parameters, six soil parameters (*m*, *Ksat_h*, *Ksat_v*, *ae*, *po*, and *gw1*) were calibrated to reproduce the observed streamflow. The six soil parameters characterize the main

soil drainage properties of both watersheds. *Ksat_v* and *Ksat_h* are vertical and horizontal saturated hydraulic, *m* is decline coefficient of Ksat with depth, *gw1* is the percentage of preferential flow from the soil surface to deep groundwater storage, *ae* is air entry pressure, and *po* is pore size index. The predictive performance of the model is evaluated using a combination of three accuracy measures: (a) Nash–Sutcliffe efficiency coefficient, R_{eff} (Nash & Sutcliffe, 1970), (b) Nash–Sutcliff efficiency coefficient with logarithmic values, R_{logeff}, and (c) the percent volume error (Son, Tague, & Hunsaker, 2016). The value of the three accuracy measures range from 0 to 1 with the perfect fit at 1. In this study, 4 years (October 1, 2004, to October 1, 2008) of streamflow data were used to calibrate soil parameters sets. To account for inherent soil parameters uncertainty in the model estimates, this study includes the soil parameter uncertainty in estimating model responses (ET and streamflow) to climate using GLUE approach (Beven & Freer, 2001). To select the behavioural soil parameter sets, the 10 best behavioural soil parameter sets (the highest streamflow accuracy) among 500 simulations were selected for the two watersheds, respectively.

2.4 | Impact of climate warming on hydrologic fluxes of TSW and SDW

This study aims to investigate the impact of climate warming on hydrologic fluxes (snow, ET, moisture deficit [MD], and streamflow) in TSW and SDW. To simulate the general direction of projected climate warming scenarios based on general circulation model (GCM) predictions for California Sierra (Cayan, Maurer, Dettinger, Tyree, & Hayhoe, 2008; Maurer & Duffy, 2005), this study adds a uniform 2 and 4 °C temperature increase to the observed meteorological record. This study applies two climate warming scenarios (2 and 4 °C) to RHESSys for the two watersheds. SDW under climate warming is compared with TSW under historical climate conditions to demonstrate the confounding effect of other hydrologic properties on each watershed's hydrologic responses to climate warming. SDW typically maintains an air temperature about 2 °C cooler than TSW (Table 1), and the two watersheds have similar total annual precipitation (Table 1). In theory, a 2 °C warming would prompt SDW to behave similarly to TSW under historical climate conditions if the difference in the climatic processes (snow and air temperature) between the two watersheds is the dominant explanation for the different hydrologic responses to warming. For this paper, we assume that snow parameters (e.g., parameters that influences melt responses to the environment), soil drainage parameters and vegetation parameters (e.g., LAI), and rooting depth) for each watershed are constant at the decadal time scale. By holding vegetation and soil properties constant, the model enables to estimate the difference in hydrologic responses to climate warming between the two watersheds (Figure 2).

The investigation examines the following hydrologic variables: interannual variation of hydrologic fluxes, seasonal ecohydrological fluxes, spatial structure of seasonal ET, and primary factors controlling seasonal spatial ET. To investigate the interannual variability of the hydrologic fluxes of the two watersheds, a long historical climate data (>50 years) is required. In TSWs and SDWs, basic climate data have been collected since 2002 and 2003, respectively. In order to extend our meteorological record to drive model scenarios, this study used the longer climate data (year 1941 to 2009) of the Grant Grove station where the station is located at 28 km away from the Bull watersheds. The Grant Grove station has a similar temporal pattern of precipitation and temperature to the Providence and the Bull climate stations. The detailed description of creating a long meteorological data is included in the Supporting Information.

This study also examines the relationship among annual precipitation, annual ET, annual MD, summer streamflow, and annual streamflow and how the relationship varies between TSW and SDW, and how climate warming alters these relationships. MD is defined as PET minus actual evapotranspiration (an index of plant water stress, (Tague, Heyn, & Christensen, 2009). Finally, this study also examines the spatial structure of monthly ET, and how the spatial structure of monthly ET changes under warming climate scenarios. The spatial structure is measured with standard deviation (*SD*) and coefficient of variance (COV). To examine the dominant factors in controlling the spatial seasonal ET both in TSW and SDW, univariate linear regression models are developed to identify the relationship between physiographic parameters and seasonal ET estimates. The Pearson correlation coefficient was used to calculate the relationship. Four physiographic parameters are considered: (a) elevation, (b) aspect, (c) LAI, and (d) wetness index (Beven & Kirkby, 1979; Table S2).

3 | RESULTS

3.1 | Snow and streamflow calibrations

Calibration of the three snow-related parameters were conducted by comparing modelled SWE and measured snow depth data (or SWE data). Calibrated temperature threshold values were (−3 to 3 °C) for both watersheds. Empirical temperature melt coefficient were (0.005 m/°C) for both watersheds. The estimated temperature lapse rates (°C m^{-1}) of two watersheds were very similar; the minimum air temperature lapse rates for TWS and SDW were −0.0064 and −0.0060, and the maximum air temperature lapse rates for TSW and SDW were 0.0063 and 0.0068, respectively.

Comparison between model estimates and measured values for days of complete snowmelt results in R^2 of 0.95, 0.9 at the Providence and Bull stations, respectively (Figure S1). These high values of R^2 imply that the model reproduced the timing of observed snowmelt (Figure S1). However, the model at the Upper Providence station underestimated SWE in the year 2004 and year 2007, and the model at the Upper Bull station underestimated the SWE in year 2004 and 2005 and overestimated SWE in the year 2008. The comparison of modelled SWE and measured SWE at the two upper station results in R^2 of 0.87 and 0.7.

Behavioural soil parameter sets are obtained comparing modelled and measured streamflow for TSW and SDW (parameter values are provided in Figure S2). In general, the model reproduced the measured

streamflow of the two watersheds. The overall accuracy of the streamflow prediction is higher for SDW than for TSW even though snow predictions in TSW are slightly better than in SDW (Table S3 and Figures S1 and S2). In SDW, the model showed high accuracy in daily flow prediction, and the high flow is better predicted than low flow (R_{eff} = 0.82–0.86 and R_{logeff} = 0.70–0.80). In TSW, the model captured the seasonal pattern of observed streamflow (Table S3), and the model had better performance for low flows than for high flows (R_{eff} = 0.47–0.56 and R_{logeff} = 0.67–0.76). The selected behavioural models showed a larger percentage error (PerErr; -23~18) in TSW than in SDW. However, the model showed relatively high streamflow accuracy values at the monthly time scales and models with the highest streamflow accuracy is less than 3% PerErr for both watersheds (Table S3).

3.2 | Climate warming's effects on interannual hydrologic responses in TSW and SDW

Figure 3 shows the relationship between annual precipitation and model estimates of annual streamflow, summer flow, annual ET, and annual MD in TSW and SDW, and the effect of warming on these relationships. Climate warming reduces annual peak SWE, annual flow, and summer flow and increases annual ET and annual MD for both watersheds (Table S4). The warming effects on these four variables are larger in SDW than in TSW. For both watersheds, 2 and 4 °C warming significantly reduced annual peak SWE compared with historical climate. In TSW, 2 and 4 °C warming results in reduction in mean annual peak SWE by 116 mm (55%) and 172 mm (82%), respectively. In SDW, 2 and 4 °C warming results in reduction

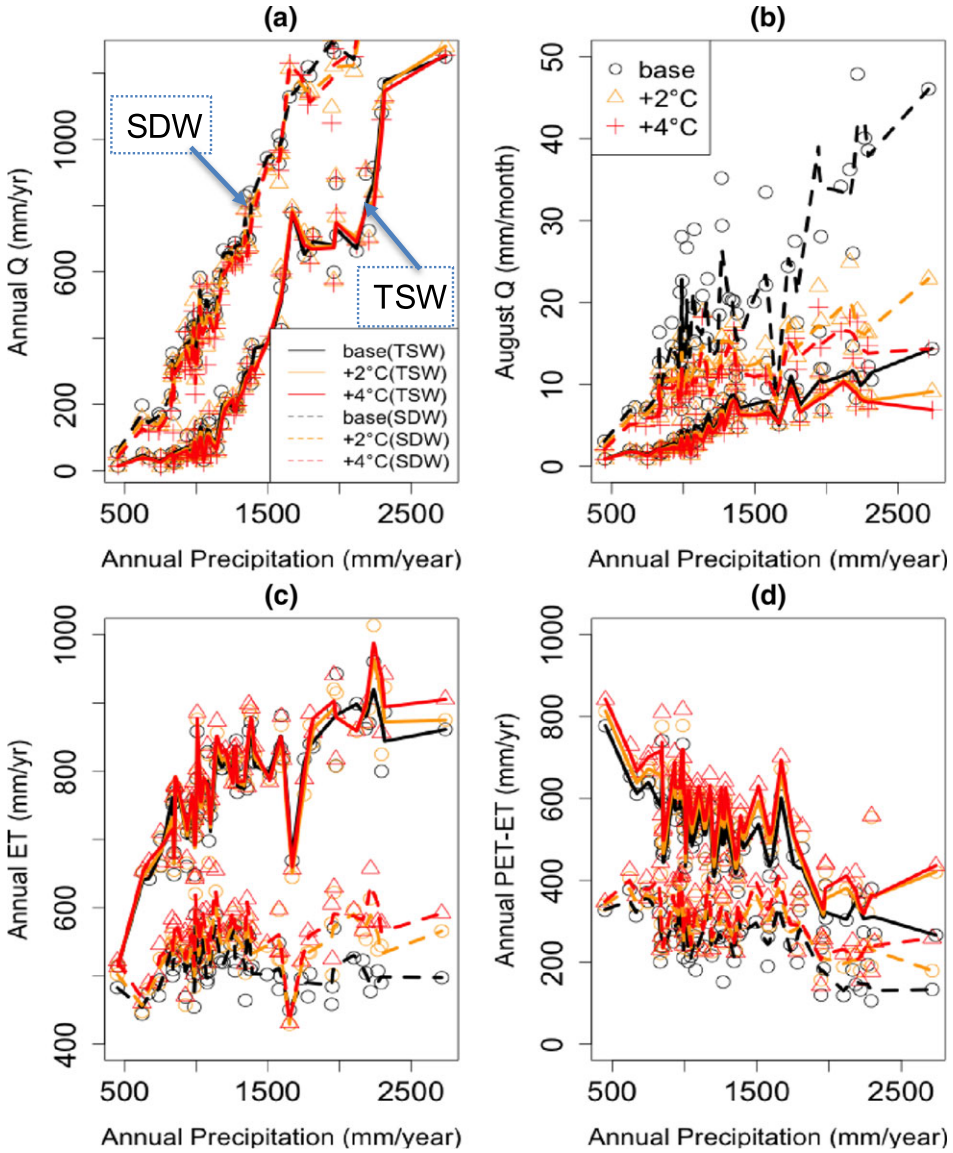

FIGURE 3 The relationship among annual precipitation, annual streamflow, August streamflow, annual moisture deficit (PET-ET), and annual ET of TSW and SDW during climate warming scenarios: (a) annual flow, (b) August (summer) flow, (c) annual ET, and (d) annual moisture deficit (PET-ET), and the three lines (black, orange, and red) were created by using LOESS (local polynomial regression fitting algorithm), and the interpolated line is used for only guiding visually the general pattern of model estimates and is not necessarily statistically significant. Sixty-four years, weighted mean (based on streamflow accuracy) of model estimates (annual streamflow, ET, summer flow, and annual moisture deficit) were plotted. ET: evapotranspiration; PET: potential evapotranspiration; SDW: snow dominated watershed; TSW: transient snow watershed

in mean annual peak SWE by 222 mm (56%) and 324 mm (81%), respectively.

For TSW, there are relatively nonlinear relationships between annual precipitation and estimated annual streamflow for baseline and warming scenarios. However, SDW has more linear relationship between annual precipitation and estimated annual streamflow. SDW has a higher run-off ratio than TSW (Figure 3a; Table 1), reflecting lower annual ET (Figure 3c and Table 1). Annual ET estimates in TSW increase nonlinearly with the increasing annual precipitation. Annual ET estimates in SDW for baseline are more or less constant with increasing precipitation, although there is substantial scatter. Both TSW and SDW show statistically significant increases in ET with 4 °C warming scenarios, and SDW shows a statistically significant increase for 2 °C as well. Relative increases in annual ET in SDW with warming are substantially greater than they are for TSW and likely reflect the greater temperature limitation in the colder SDW. However, as noted above, these increases are not sufficient to bring annual ET in SDW to baseline annual ET for TSW. Both watersheds show greater increases in annual ET with warming in wetter years, although this effect is small relative to interannual variation in annual ET. For SDW, under the 4 °C warming scenario, there is some suggestion of a stronger relationship between annual ET and annual precipitation such that the relationship is becoming more similar to the shape (though not magnitude) of this relationships for TSW.

Annual MD estimates in TSW decrease with increasing precipitation with a steeper slope than those in SDW. These results suggest that TSW is a more water-limited watershed than SDW. Warming significantly increases mean annual MD (Table S4) for all scenarios, but the increase is substantially greater for SDW (16% vs. 8% and 23% vs. 13% for 2 and 4 °C). Nonetheless, annual MD for SDW remains well below that of TSW, even when comparing 4 °C warming in SDW with baseline TSW scenarios.

>Summer flow estimates for both watersheds have positive relationships with the annual precipitation. SDW has higher magnitude and variability of summer flow than TSW. Summer flow shows the greatest relative (percent) change with warming for both watersheds, relative to other ecohydrologic variables. This is particularly true for SDW. Summer flow reductions for SDW are greater than those for TSW and summer flows estimates for 4 °C for SDW beginning to approach the summer flow magnitude for baseline TSW. For SDW, slope of the relationship between summer flow and precipitation substantially declines between baseline and 2 °C warming and is more similar to this slope for TSW.

3.3 | Climate warming's effects on seasonal hydrologic responses in TSW and SDW

Figure 4 shows the effect of climate warming on monthly SWE, ET, MD, and streamflow in the two watersheds. As with annual fluxes, the effects of warming on the monthly hydrologic fluxes in SDW are larger than those in TSW. In TSW, peak monthly SWE occurs in March, and climate warming decreases snow accumulation and accelerates snowmelt (Figure 4a). For a 2 °C warming, SDW has the same timing but slightly smaller magnitudes of monthly SWE as TSW under historical climate conditions. With a 4 °C warming, most precipitation occurs as rain rather than snow for both TSW and SDW.

In TSW, peak monthly ET occurs in May, and 2 and 4 °C warming do not change this timing but increases monthly ET in the winter and early spring while decreasing monthly ET in the late spring and summer. A 2 °C warming in SDW does shift the timing of peak monthly ET from June to May, but the change in the magnitude of peak monthly ET is less than 5%. A 2 °C warming increases monthly ET from October to May but decreases monthly ET in all other months. With a 2 °C warming, SDW has similar temporal monthly ET patterns to TSW under historical climate conditions, although peak and total ET remains substantially higher for TSW.

Peak monthly MD occurred in August for both TSW and SDW for baseline and 2 and 4 °C warming scenarios. For both TSW and SDW, warming increases the monthly MD from May to November and decreases the monthly MD in all other months.

For TSW, peak monthly streamflow occurs in March for all scenarios, and at a daily time step, there is 12 and 15 day shift in timing of flow to earlier in the year (measured as centre of mass of flow) for 2 and 4 °C warming scenarios. A 2 °C warming does increase peak monthly streamflow magnitude from 66 to 72 mm. Warming increases the monthly streamflow in January to March and decreases the monthly streamflow in the remaining months. For SDW, peak monthly streamflow occurs in May under historical climate conditions, but peak monthly streamflow shifts to March under 2 and 4 °C warming scenarios, and at a daily time step, there is 37 and 45 day shift timing for flow to earlier in the year (measured as centre of mass of flow). The shift in timing of peak streamflow is much greater for SDW when a 2 °C warming is applied. With a 2 °C warming, the timing of SDW's peak monthly streamflow shifts to dates similar to TSW under historical climate conditions, and the magnitude of SDW's peak monthly streamflow decreases from 153 to 139 mm; however, SDW under 2 °C warming still simulates larger monthly streamflow than TSW under historical climate conditions.

3.4 | Climate warming's effects on spatial structure of seasonal ET and its relationship with physiographic parameters

Figure 5 shows the effect of climate warming on the spatial structure of monthly ET in TSW and SDW. Both TSW and SDW show increasing *SD* and COV in ET throughout the spring, with peak spatial variation occurring late in the summer followed by declines (Figure 5a). For the historic climate scenario, the *SD* of ET peaks slightly earlier for TSW (July vs. August). SDW has a lower *SD* of spatial ET in the spring and winter compared with TSW. In TSW, 2 and 4 °C warming decreases the spatial *SD* of ET in the spring and increases the spatial *SD* of ET in the summer. However, in SDW, 2 and 4 °C warming increases *SD* of ET in the winter, spring, and summer. SDW under 2 °C warming has similar temporal patterns of *SD* of spatial ET to TSW under historical climate conditions, and both watersheds have the highest *SD* in July. SDW under 2 °C warming however continues to project a higher *SD* of spatial ET in the

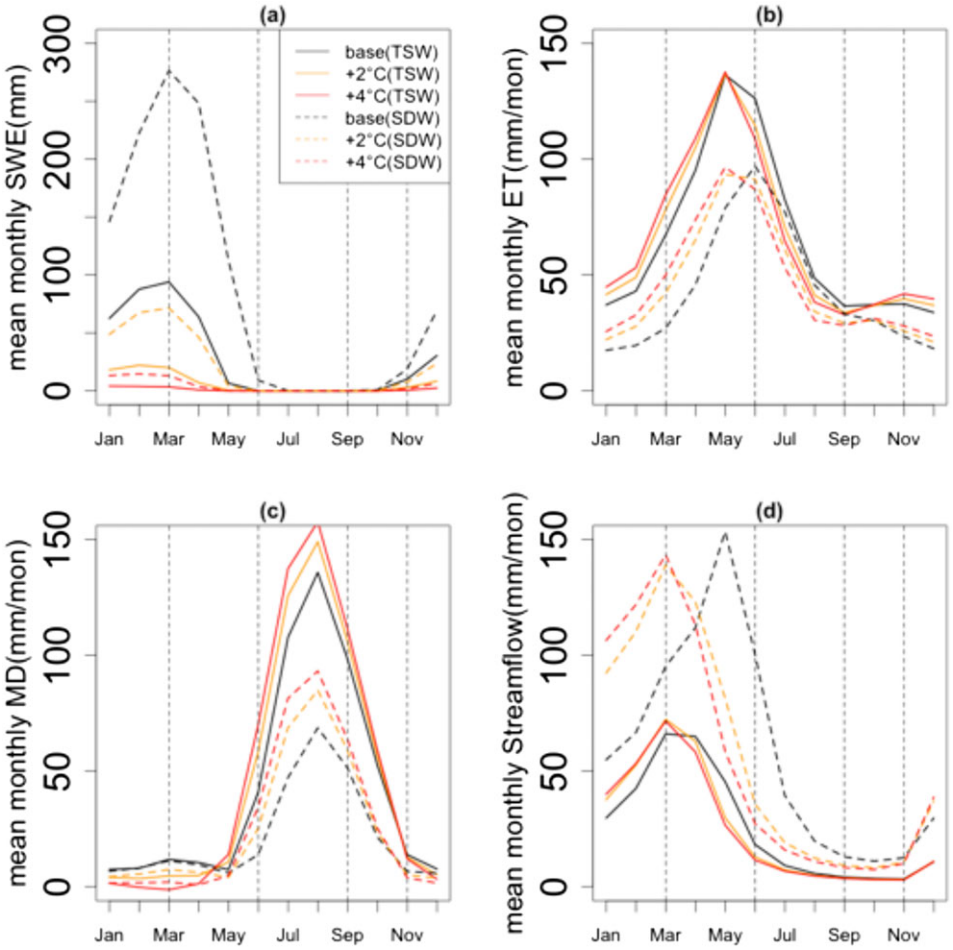

FIGURE 4 Climate-warming effect on long period (64 years) seasonal hydrologic fluxes of TSW and SDW: (a) monthly mean flow across 64 years, (b) monthly mean ET across 64 years, (c) monthly mean moisture deficit across 64 years, and (d) monthly mean streamflow across 64 years. Sixty-four years, weighted mean (based on streamflow accuracy) of model estimates (annual streamflow, ET, summer flow, and annual moisture deficit) were used to calculate the mean monthly averaged values. ET: evapotranspiration; SDW: snow dominated watershed; TSW: transient snow watershed

summer and lower *SD* of spatial ET in the spring than TSW under historical climate conditions.

Both watersheds have the highest COV of spatial ET in August under historical climate conditions (Figure 5b). Climate warming decreases COV of spatial ET in the winter and early spring but increases its values in the summer for both watersheds. The highest COV of spatial ET occurs in the August under the two warming scenarios. SDW under 2 °C warming has similar temporal patterns of COV of spatial ET and higher COV values, compared with TSW under historical climate conditions.

Figure 6 shows the relationship between four physiographic parameters and spatial monthly ET in TSW and SDW and the warming effect on these relationships. In TSW, elevation has negative correlation with ET in the winter and spring and has positive correlations with ET in the summer (Figure 6a). Lower elevations tend to have higher ET due to higher temperatures. Aspect has negative correlation with ET in most months, such that southwest locations tend to have higher ET (Figure 6b). Because slopes with southwest aspect tend to receive more radiation, and have earlier snowmelt, southwest slopes will tend to have higher ET in the winter and spring. As the season changes to summer, effect of aspect becomes minor. Wetness index always has positive correlation with ET, and in summer, the wetness index has the highest correlation with spatial ET among the four physiographic parameters. LAI has positive and the highest correlation values with ET in winter, spring, and fall. The correlation between ET and LAI decreases in the summer. Lower correlation between ET and LAI in the summer reflect the impact of water stress on ET, particularly for higher LAI sites.

The relationships between physiographic parameters and spatial monthly ET in SDW are very similar to those in TSW. Elevation and aspect have a negative correlation with spatial ET in the winter and in the spring, and the correlation values become closer to zero in the summer. Wetness index always shows positive correlation with ET, and correlations are higher in summer than other seasons. SDW has a notably higher correlation with wetness index during the spring and summer than TSW. Similar to TSW, LAI has a positive correlation with ET and the highest correlation value, across all physiographic parameters, with spatial ET in the winter, the spring, and the fall. As with the TSW, the correlation between spatial ET and LAI decreases in the summer, although SDW maintains higher correlations in June or July relative to TSW.

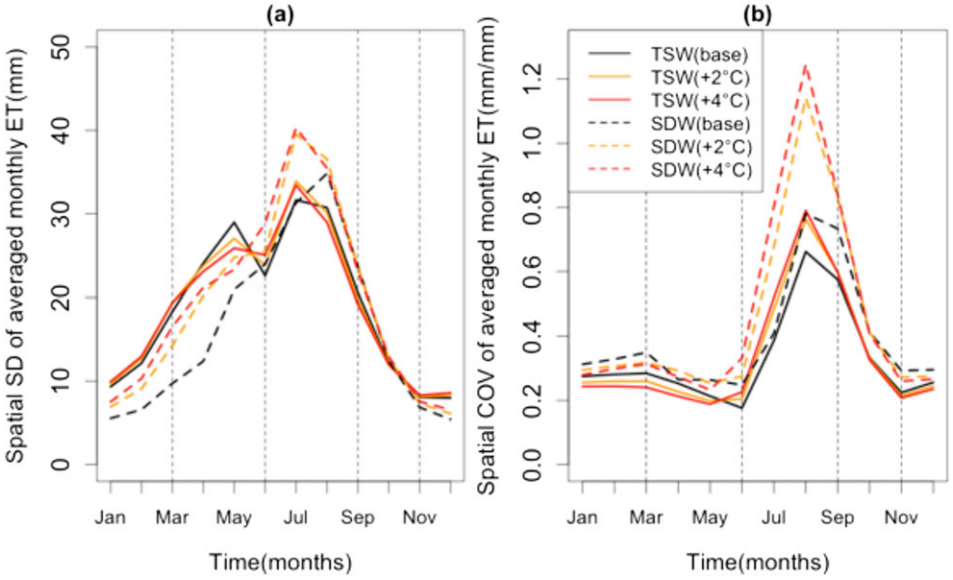

FIGURE 5 Spatial standard deviation (*SD*), coefficient of variance (COV) of monthly ET across 64 years for TSW and SDW with climate warming: (solid line) TWS and (dotted line) SDW: (a) spatial *SD* of averaged monthly ET and (b) spatial variance (COV) of averaged monthly ET

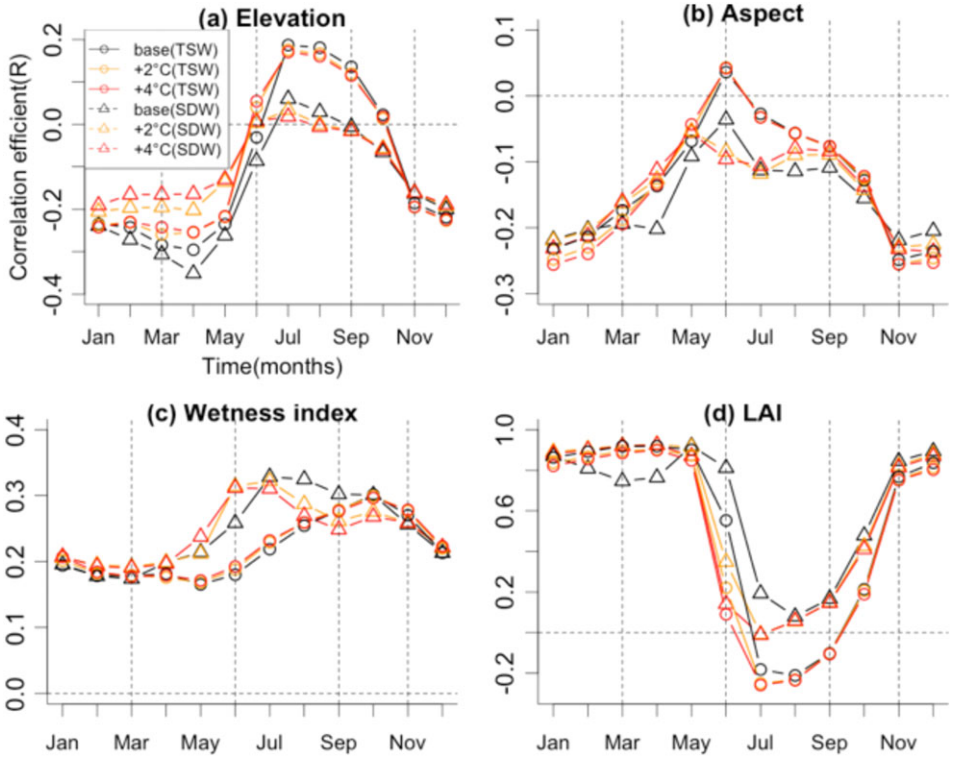

FIGURE 6 The relationship between physiographic parameters and the spatial pattern of monthly ET (expressed as Pearson correlation coefficient [*R*]): (a) elevation, (b) aspect, (c) wetness index, and (d) LAI. ET: evapotranspiration; LAI: leaf area index

The effects of warming on the relationship between monthly ET and physiographic parameters are larger in SDW than in TSW. Under 2 °C warming, the correlation between wetness index and ET in SDW increases in the spring but decreases in the summer. Effect of warming on these relationships in TSW is minor. Thus, the change in wetness index and ET relationships for SDW with a 2 °C warming does not result in a temporal pattern that is more similar to TSW. The consistently greater correlation with wetness index early in the season in SDW relative to TSW, even under warming scenarios, likely reflects the impact of cross-correlations between LAI and wetness index that are greater in SDW (Table S3). The correlation values between LAI and ET in SDW increase in the winter and early spring, but the values decrease in late spring and the summer and begin to resemble low LAI-ET correlations for TSW. In TSW, the correlation between LAI and ET slightly decreases or remains constant. Warming reduces the correlation between LAI and summer ET in both

watersheds. In SDW, the increase of available water for plant due to earlier snowmelt and change in the precipitation phase from snow to rain can explain the increase in correlation between monthly ET and LAI in the winter and earlier spring. The increase in water limitation due to the higher vapour deficit in atmosphere and higher MD in soil lead to the decreased correlation values in the summer for both watersheds. Although SDW under 2 °C warming has higher correlation value in the monthly ET and LAI than TSW under historical climate conditions, especially in winter and spring, the two watersheds have a similar temporal pattern in the relationship between monthly ET and LAI. These relationships in SDW are very similar under 2 and 4 °C warming scenarios.

4 | DISCUSSION

This study uses a process-based hydrologic model, RHESSys to examine the potential difference in hydrologic changes between TSW and SDW for climate warming scenarios. In particular, we examine whether a 2 °C warming in the SDW, which leads to mean annual temperatures in SDW that are similar to those in TSW under historic climate, also leads to similar ecohydrology fluxes. Results show that although warming does shift ecohydrologic fluxes in SDW towards the magnitude, seasonality and spatial pattern of those associated with TSW, differences remain between the two watersheds in their sensitivity to climate drivers.

4.1 | Model performance and uncertainty

In RHESSys, snow parameters and soil parameters were calibrated to represent the hydrologic processes in the two watersheds. In some years, the model prediction of SWE did not match observed snow data. One major problem may be related to estimating the fraction of snow in the total precipitation. In the RHESSys, two fixed temperature threshold values are used to partition the precipitation into snow and rain, and the temperature threshold may vary with events, season, and year (Marks et al., 2013). Previous studies showed that hourly humidity-based methods and physical precipitation-phase partitioning methods are a better predictor for the precipitation phase than daily temperature-based methods (Marks et al., 2013). The lower model accuracy in the Upper Bull station (Figure 3d) may be related to measurement errors in SWE (Johnson & Schaefer, 2002). This study however focuses how different snow processes in the two watersheds may affect the sensitivity of hydrologic responses to climate warming. Because the modelled SWE is able to mimic the difference in the timing and magnitude of snow accumulation and melt between the two watersheds, the error of the SWE prediction will not influence this study conclusion. In addition, model misrepresented some peak observed flow. The poor prediction of peak flow may be due to an overestimation of the fraction of snowfall in total precipitation in late fall and in winter as well as misrepresentation of variable soil depth within the watershed. TSW has areas with locally shallow soil depths (Bales et al., 2011). These areas with shallow depths can generate the peak flow rapidly responding to snowmelt or rainfall event. In this study, soil depth is assumed to be uniform within the watershed because detailed soil depths map at fine scales were not available at the time of this study. The model performance is also similar to performance statistics obtained for other hydrologic model applications in this region (Cristea, Lundquist, Loheide, Lowry, & Moore, 2014; Tague & Peng, 2013). Based on this level of model performance, we suggest that the calibrated model can be used to test the difference in the sensitivity of seasonal and annual model estimates to climate warming between the two watersheds.

4.2 | Effects of climate warming on hydrologic fluxes

As expected, modelling results showed that increasing air temperature reduces snow accumulation and accelerates snowmelt, increases annual ET, and decreases annual streamflow and summer flow in both TSW and SDW. These results are consistent with previous modelling and empirical studies in snow dominated mountain regions (Berghuijs, Woods, & Hrachowitz, 2014; Christensen et al., 2008; Godsey, Kirchner, & Tague, 2014; Tague et al., 2009). The reductions of annual streamflow and summer flow result from the reduction of SWE and the increase of spring ET.

Modelling results showed that SDW has higher sensitivity to climate warming than TSW for mean and for seasonal and spatial variation in ecohydrologic fluxes. In general, this greater sensitivity reflects an elevation-based transition between a more water-limited site (TSW) and a more temperature-limited site (SDW). SDW shows a greater reduction in snow accumulation and greater increases in spring ET. Increases in ET with warming in TSW on the other hand are limited by available water, and thus, although there are increases in spring ET, these increases are smaller than those in SDW and are balanced by greater water limitation declines in summer ET with warming (Figure 4). We note however that both watersheds show summer water limitations with warming scenarios and greater gains in ET with warming in wet years (Figure 3). The empirical study of Goulden and Bales (2014) of current ET fluxes across elevation gradients in the Sierra are consistent with these results. Goulden and Bales (2014) used flux tower ET data and MODIS vegetation product normalized difference vegetation index (NDVI) in upper King River Basin to show that above 2,400 m, estimated ET is limited by cold temperatures, whereas at lower elevations, estimated ET is limited by water availability. Consequently, the sensitivity of ET to warming is more significant at the higher elevations than at the lower elevations.

4.3 | Does 2 °C warming makes SDW to behave hydrologically similar to TSW under historical climate conditions?

Shifts in snow, streamflow, and ET with warming in SDW generally result in fluxes that are more similar to those of TSW. However, the magnitude of these changes was not sufficient to fully compensate for prewarming differences between the two watersheds (Table 2).

When 2 °C warming is applied to SDW, SDW has a similar mean air temperature and monthly SWE patterns in comparison with TSW (Table 2). However, there are still differences in hydrological behaviour between the two watersheds. With 2 °C warming, SDW still has higher annual streamflow and summer flow than TSW under historical climate conditions (Table 2). Further, even though warming increases annual ET in SDW in wet periods, the slope of the annual ET versus annual precipitation curve in SDW is still small compared with this slope in TSW (Figure 3). Thus, lower annual ET, and higher annual or summer run-off associated with SDW must, therefore, be attributed to other differences included the model implementation. A key difference is the greater mean LAI in TSW (2.6 vs. 1.2), which likely supports both higher rates of canopy evaporation and transpiration.

Model estimates of ET in RHESSys account for the interaction among atmospheric process, soil water availability, and tree physiology. Warming increases atmospheric demand by increasing the capacity of air to hold moisture and changes the timing of water inputs to the soil by changing snowmelt. In the model implementation used here, vegetation parameters (e.g., LAI and rooting depth) were held constant, and both LAI and rooting depth are lower in SDW. Lower LAI for trees in SDW means that they experience less frequent water stress conditions compared with those in TSW even after snow processes and atmospheric demand for ET became similar with a 2 °C warming. To examine how a shift in LAI in SDW might alter these results, we perform additional simulation to test the effect of LAI on the responses of annual ET and annual MD to precipitation in SDW. Figure 7 and Table 3 show the effect of doubling LAI in SDW under 2 °C warming scenario on annual ET and annual MD. A doubling of LAI in SDW leads to an LAI in SDW similar to the LAI in TSW. Doubling the LAI in SDW under 2 °C warming increases annual ET, and slope of the annual ET versus annual precipitation curve becomes similar to the slope in TSW under historical climate condition. Doubling the LAIs in SDW increases annual MD and yields values that are similar to annual MD in TSW. Thus, once differences in LAI are accounted for, SDW for the 2 °C warming scenario are more similar to hydrologic fluxes for TSW under baseline conditions. However, SDW under 2 °C warming with mean LAI value similar to TSW has lower mean annual ET (119 mm, 15%) than TSW under historical climate conditions. Shallower rooting depth in SDW may attribute to the lower ET. In this study, 2-m rooting depth was applied to TSW, whereas 1-m rooting depth was applied to SDW. These results suggest that the differences in vegetation structures between the two watersheds can partially explain the different ET response to climate warming.

When doubling LAI and 2 °C warming are applied to SDW, SDW still generates higher annual flow and summer flow than TSW under historical climate conditions (Table 3). The difference of subsurface properties between the two watersheds may explain the remaining flow difference. Even though the two watersheds have the same granitic geology, TSW has more deeply weathered bedrock than SDW (Dahlgren, Boettinger, Huntington, & Amundson, 1997). TSW therefore has higher percolation in deep groundwater storage through preferential flow paths than SDW. Calibrated drainage parameters in RHESSys for the two watersheds reflect these geologic distinctions (Table S1); SDW has higher *Ksat_h* value and lower *gw1* than TSW. SDW with relatively shallow regolith depths therefore can generate faster subsurface flow. Due to the difference of subsurface properties and vegetation structures, SDW under 2 °C warming still generates higher annual flow and summer flow compared with TSW under historical climate conditions. Previous studies using empirical approach improve our understanding of the sensitivity of ET and streamflow

TABLE 2 Comparison between SDW under 2 °C warming and TSW under historical climate conditions in terms of hydrologic responses to climate

Question: Does SDW under 2 °C warming behave similar to TSW under historical climate condition?			
Variable	**Spatial scale/time scale**	**SDW ≈ TSW**	**Comments**
Snow	Mean watershed/month	Yes	The timing of peak monthly SWE is same, but TSW has higher peak monthly SWE than SDW.
ET	Mean watershed/annual	No	SDW has lower annual ET than TSW, and SDW experiences water limitation less often than TSW.
	Mean watershed/month	Yes	The two watersheds have same timing of peak monthly ET, but TSW has lower monthly ET than SDW.
	SD of watershed/month	Yes	The highest spatial variance (*SD*) in monthly ET occurs in July for the two watersheds, but SDW has higher *SD* than TSW.
	COV of watershed/month	Yes	Two watersheds have similar temporal pattern of COV in monthly ET but SDW has higher COV.
	Patch level/month in the relationship with physiographic parameters	No	LAI and wetness index are main factors controlling the seasonal ET in the both watersheds, but 2 °C warming does not make the relationship between physiographic parameters and ET in SDW to be similar to those in TSW under historical climate.
MD	Mean watershed/annual	No	SDW has lower MD than TSW.
	Mean watershed/month	Yes	The two watersheds have same timing of peak monthly ET, but TSW has higher monthly MD.
Streamflow	Mean watershed/annual	Yes	The two watersheds have similar relationship between annual flow and annual precipitation, but SDW always has higher annual streamflow.
	Mean watershed/month	Yes	The two watersheds have same timing of peak monthly streamflow, but SDW has higher monthly streamflow.
August streamflow	Mean watershed/annual	Yes	The two watersheds have similar relationship between summer flow and annual precipitation, but SDW has higher summer streamflow.

Note. COV: coefficient of variance; ET: evapotranspiration; MD: moisture deficit; SD: standard deviation; SDW: snow dominated watershed; SWE: snow water equivalent; TSW: transient snow watershed.

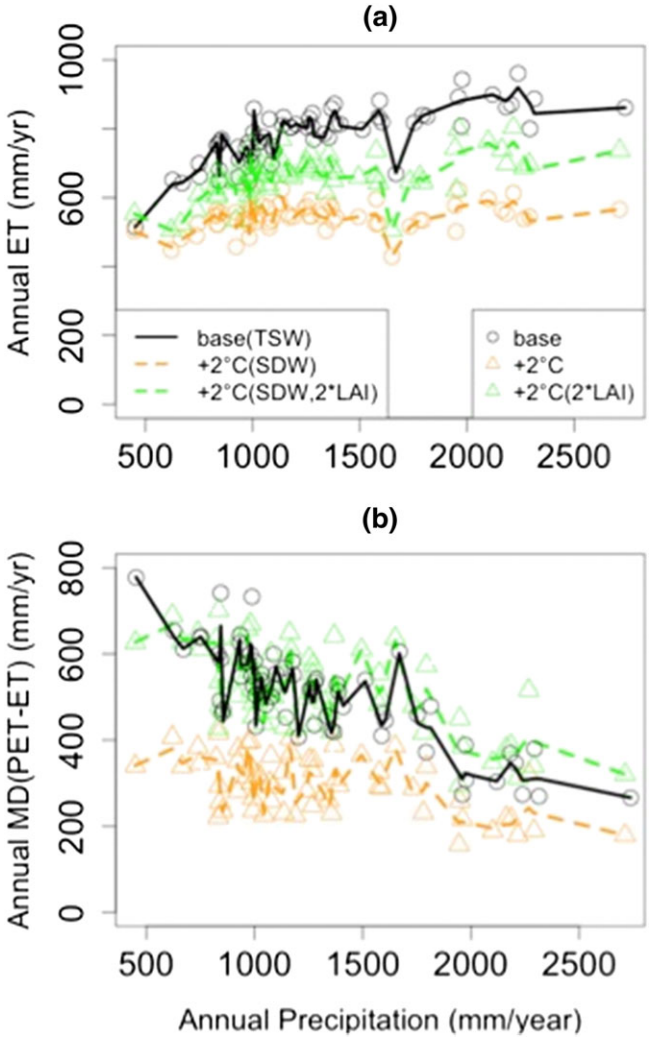

FIGURE 7 The relationship between annual precipitation, annual evapotranspiration (ET), and annual moisture deficit (MD) in TSW and SDW: (a) annual ET and (b) annual MD (PET-ET). There are two scenarios for SDW including 2 °C warming and doubled LAI value. Using LOESS (local polynomial regression fitting algorithm) created the three lines (black, orange, and green). PET: potential evapotranspiration; SDW: snow dominated watershed; TSW: transient snow watershed

TABLE 3 Comparisons of annual water budget between TSW under historical climate conditions and SDW under 2 °C climate warming scenarios and under change in vegetation structure

	TSW	SDW
	Historical climate conditions	2 °C warming + 2*LAI
Annual Streamflow (mm)	304	562 (85%)[a]
Summer Streamflow (mm)	5.8	10 (72%)
Annual ET (mm)	781	662 (15%)
Annual MD (mm)	502	517 (3%)

Note. LAI: leaf area index; SDW: snow dominated watershed; TSW: transient snow watershed.

[a]Parentheses show the percentage ratio of each flux for SDW to each flux for TSW.

to climate warming in various sites (Jefferson, 2011; Nolin & Daly, 2006; Safeeq et al., 2013). However, empirical approaches have difficulty in assessing the effect of climate warming on individual watersheds due to the confounding effect of other landscape properties (Peel & Bloschl, 2011). Here, we show that although temperature differences are an important control on ecohydrologic differences along an elevation gradient—difference in vegetation and subsurface geology can lead to responses to climate warming that diverge from expectations based solely on a substitution along elevation-based temperature gradients.

Although the two watersheds have substantial differences in magnitude of annual hydrologic fluxes and their sensitivity to warming, in seasonal hydrologic fluxes including monthly SWE, ET, and streamflow patterns, SDW under 2 °C warming scenario behaves similar to TSW under historical climate (Table 2; Figure 4). For example, the two watersheds have the same timing of monthly SWE and peak monthly ET, MD, and streamflow. The temporal pattern in *SD* of monthly ET in SDW under climate warming is similar to those in TSW under historical climate conditions. The similar response of the two watersheds can be attributed to the temporal distribution of water and energy in the two watersheds: in both watersheds, winter precipitation in annual precipitation is dominant, and solar radiation and air temperatures have similar temporal patterns.

4.4 | The spatial structure of ET and the relationship between the physiographic parameters and spatial ET

This modelling study showed that LAI is the dominant control on the spatial ET for most of the year and for both watersheds, and wetness index becomes important during the summer in both watersheds, and these patterns remain under future warming conditions. Interestingly, these two parameters are dominant over elevation and aspect as controls on spatial patterns of model estimates of ET. In mountain watersheds, elevation is highly correlated with air temperature and precipitation, and aspect is also highly correlated with solar radiation distribution. However, the two watersheds in this study have a low spatial variability (less than 1%) of precipitation along elevation gradients. Low temperature gradient is also observed due to small elevation range, compared with other studies (Christensen et al., 2008; Tague et al., 2009). In regions drier than our sites, aspect may play a key role in controlling vegetation water use and growth through large solar irradiance differences. Goulden and Bales (2014) showed that the effect of local aspect on estimated ET (NDVI-based ET) is more substantial in the lower elevation (<1,000 m) in King River Basin where the water limitation is a key controls on vegetation behaviours. Aspect within both watersheds tends to have a unimodal distribution rather than bimodal distribution (Son et al., 2016). These environmental limitations and spatial pattern of aspect explain the low correlation between aspect and spatial ET in this watershed.

Our modelling study showed that spatial variances (*SD* and COV) of monthly ET are highest in the summer. Kerkez et al. (2012) in a soil moisture sampling study, conducted in a subwatershed (P301) of TSWs found similar results where soil moisture variation (COV) increases in the summer period. Climate warming also increases the spatial variances, although this effect is small relative to differences

between months or between watersheds. The relationships between mean soil moisture and variance in soil moisture often have a nonlinear form, and their form varies depending on the climate, topography, and vegetation (Lawrence & Hornberger, 2007; Teuling, 2005). In these watersheds, the spatial variation in ET reflects temporal change in limiting factors associated with a Mediterranean climate. In the winter, ET is low throughout the watershed, as temperatures warm ET increases and areas that have higher LAI or warmer temperatures have relatively greater ET and thus increase spatial variance. Once moisture limitation begins to occur, ET is reduced. This reduction will preferentially occur in drier areas (low wetness index) or areas with higher LAI that use water more quickly. Note that in the summer, the wetness index shows the highest correlation with ET across physiographic factors. Thus, water limitation initially increases spatial variation, but ultimately, as the season progresses and water limitation occurs consistently throughout the watershed, spatial variation in ET decreases. The result is spatial variation in ET that peaks in August for both watersheds. The greater increase in spatial variation in ET particularly as COV for SDW, which is less water limited, is somewhat surprising but reflects how spatial variation in moisture limitation and LAI interact. ET maintains a positive correlation with LAI for SDW even in late summer, and LAI and wetness index are correlated in SDW. These two factors maintain a higher spatial variation in ET in SDW, where, in this less water limited system, higher LAI has higher ET even in the summer. The correlation between LAI and ET is negative for TSW in the summer, suggesting that (a) the primary cause of spatial variation is water stress and (b) the greater and more spatial ubiquitous summer water stress reduction in ET in TDW ultimately limits the maximum spatial variation. These results illustrate the complexity of within watershed patterns spatial patterns of ET, showing how it is the combination of LAI, water limitations and temperature that lead to the evolution of spatial variance throughout the season. Finally, we also note that model estimates of COV are greater than 50% for both watersheds during the summer emphasizing that monitoring of vegetation summer water stress may require dense sampling networks.

5 | CONCLUSION

This study illustrates the similarity and dissimilarity between TSW and SDW in terms of the climate warming's effect on hydrologic cycles. These differences offer a mechanistic explanation of watershed sensitivity to climate warming and show that although elevation based shifts from water limited to temperature limited forests are key controls—vegetation structure (LAI) and geologic differences also influence sensitivity. Patterns of LAI and within watershed drainage (indicated by wetness index) are also a primary factor controlling spatial patterns of seasonal ET, under both historical climate conditions and climate warming scenarios. Spatial variation in ET in both watersheds increases during the spring and peaks in midsummer. The physiographic factors controlling this pattern however differ between the more water limited TSW and temperature limited SDW and also reflect difference in current LAI patterns and drainage characteristics in the two watersheds. For both watersheds, warming will likely increase spatial variation in ET, although for different reasons. Although these results are specific to these watersheds, we expect that similar types of relationships among climate, topographic, and vegetation drivers across the Sierra and this detailed mechanistic modelling study offers insight into interrelationships between these variables. These results have implications on how we manage these watersheds in a warming climate, particularly for forest managers who must target limited resources for fuel treatments and other efforts. Forest ET is broadly used as indicators of water stress (Stephenson & van Mantgem, 2011; Williams et al., 2012), and thus, understanding how spatial patterns of ET evolve and the mechanisms that reflect this are important for developing spatially explicit management plans.

ACKNOWLEDGEMENTS

We gratefully acknowledge the data collected by Kings River Experimental Watershed Project (KREW) and two anonymous reviewers for providing helpful comments on a previous version of this manuscript. This study was financially supported by Southern Sierra Critical Zone Observatory Project from National Science Foundation (EAR-0725097). The opinions, findings, conclusions, or recommendations expressed in the material are those of the authors and do not necessarily reflect the views of the National Science.

Foundation.

ORCID

Kyongho Son http://orcid.org/0000-0003-0288-6522

REFERENCES

Bales, R. C., Hopmans, J. W., O'Geen, A. T., Meadows, M., Hartsough, P. C., Kirchner, P., … Beaudette, D. (2011). Soil moisture response to snowmelt and rainfall in a Sierra Nevada mixed-conifer forest. *Vadose Zone Journal*, *10*(3), 786. https://doi.org/10.2136/vzj2011.0001

Berghuijs, W. R., Woods, R. A., & Hrachowitz, M. (2014). A precipitation shift from snow towards rain leads to a decrease in streamflow-supplement. *Nature Climate Change*, *4*(7), 583–586. https://doi.org/10.1038/NCLIMATE2246

Beven, K., & Freer, J. (2001). Equifinality, data assimilation, and uncertainty estimation in mechanistic modelling of complex environmental systems using the GLUE methodology. *Journal of Hydrology*, *249*, 11–29 Available at: http://www.sciencedirect.com/science/article/pii/S0022169401004218. https://doi.org/10.1016/S0022-1694(01)00421-8

Beven, K., & Kirkby, M. J. (1979). A physically based, variable contributing area model of basin hydrology/Un modèle à base physique de zone d'appel variable de l'hydrologie du bassin versant. *Hydrological Sciences Bulletin*, *24*(1), 43–69. https://doi.org/10.1080/02626667909491834

Cayan, D. R., Maurer, E. P., Dettinger, M. D., Tyree, M., & Hayhoe, K. (2008). Climate change scenarios for the California region. *Climatic Change*, *87*(S1), 21–42. https://doi.org/10.1007/s10584-007-9377-6

Christensen, L., Tague, C., & Baron, J. (2008). Spatial patterns of simulated transpiration response to climate variability in a snow dominated mountain ecosystem. *Hydrological Processes*, *22*, 3576–3588. https://doi.org/10.1002/hyp

Clapp R, Hornberger G. 1978. empirical equations for some soil hydraulic properties. Water Resources Research **14** (4) Available at: https://doi.org/10.1029/WR014i004p00601/full [Accessed 28 October 2014]

Cristea, N. C., Lundquist, J. D., Loheide, S. P., Lowry, C. S., & Moore, C. E. (2014). Modelling how vegetation cover affects climate change impacts on streamflow timing and magnitude in the snowmelt-dominated upper Tuolumne Basin, Sierra Nevada. *Hydrological Processes*, *28*(12), 3896–3918. https://doi.org/10.1002/hyp.9909

Dahlgren, R., Boettinger, J. L., Huntington, G. L., & Amundson, R. G. (1997). Soil development along an elevational transect in the western Sierra Nevada, California. *Geoderma*, *78*(3–4), 207–236. https://doi.org/10.1016/S0016-7061(97)00034-7

Glassy, J., & Running, S. (1994). Validating diurnal climatology logic of the MT-CLIM model across a climatic gradient in Oregon. *Ecological Applications*, *4*(2), 248–257 Available at: http://www.jstor.org/stable/1941931 . https://doi.org/10.2307/1941931Accessed 25 September 2014

Godsey, S. E., Kirchner, J. W., & Tague, C. L. (2014). Effects of changes in winter snowpacks on summer low flows: case studies in the Sierra Nevada, California, USA. *Hydrological Processes*, *28*(19), 5048–5064. https://doi.org/10.1002/hyp.9943

Goulden, M. L., & Bales, R. C. (2014). Mountain runoff vulnerability to increased evapotranspiration with vegetation expansion. *Proceedings of the National Academy of Sciences*, *111*(39), 14071–14075. https://doi.org/10.1073/pnas.1319316111

Howat, I. M., & Tulaczyk, S. (2005). Climate sensitivity of spring snowpack in the Sierra Nevada. *Journal of Geophysical Research*, *110*(F4), F04021. https://doi.org/10.1029/2005JF000356

Hunsaker, C. T., Whitaker, T. W., & Bales, R. C. (2012). Snowmelt runoff and water yield along elevation and temperature gradients in California's Southern Sierra Nevada[1]. *JAWRA Journal of the American Water Resources Association*, *48*(4), 667–678. https://doi.org/10.1111/j.1752-1688.2012.00641.x

Hwang T, Band L, Hales TC. 2009. Ecosystem processes at the watershed scale: Extending optimality theory from plot to catchment. Water Resources Research **45** (11): n/a--n/a. https://doi.org/10.1029/2009WR007775

Jarvis, P. G. (1976). The interpretation of the variations in leaf water potential and stomatal conductance found in canopies in the field. *Philosophical Transactions of the Royal Society, B: Biological Sciences*, *273*(927), 593–610. https://doi.org/10.1098/rstb.1976.0035

Jasper, K., Calanca, P., & Fuhrer, J. (2006). Changes in summertime soil water patterns in complex terrain due to climatic change. *Journal of Hydrology*, *327*(3–4), 550–563. https://doi.org/10.1016/j.jhydrol.2005.11.061

Jefferson AJ. 2011. Seasonal versus transient snow and the elevation dependence of climate sensitivity in maritime mountainous regions. Geophysical Research Letters **38** (16): a. https://doi.org/10.1029/2011GL048346

Johnson, J., & Schaefer, G. (2002). The influence of thermal, hydrologic, and snow deformation mechanisms on snow water equivalent pressure sensor accuracy. *Hydrological Processes*, *3542*(August), 3529–3542. https://doi.org/10.1002/hyp.1236

Kerkez, B., Glaser, S. D., Bales, R. C., & Meadows M. W. (2012). Design and performance of a wireless sensor network for catchment-scale snow and soil moisture measurements. *Water Resources Research*, *48*(9), W09515.

Kim E, Kang S, Lee B. 2007. Parameterization and application of Regional Hydro-Ecologic Simulation System (RHESSys) for integrating the eco-hydrological processes in the Gwangneung Headwater Catchment. *Korean Journal of Agricultural and Forest Meteorology*. 9 (2): 121–131 Available at: http://agris.fao.org/agris-search/search.do?recordID=KR2008001715 [Accessed 3 December 2014]

Klos, P. Z., Link, T. E., & Abatzoglou, J. T. (2014). Extent of the rain-snow transition zone in the western U.S. under historic and projected climate. *Geophysical Research Letters: N/a-N/a*, *41*, 4560–4568. https://doi.org/10.1002/2014GL060500

Lawrence, J. E., & Hornberger, G. M. (2007). Soil moisture variability across climate zones. *Geophysical Research Letters*, *34*(20), L20402. https://doi.org/10.1029/2007GL031382

Mackay, D. S., Samanta, S., Nemani, R. R., & Band, L. E. (2003). Multi-objective parameter estimation for simulating canopy transpiration in forested watersheds. *Journal of Hydrology*, *277*, 230–247. https://doi.org/10.1016/S0022-1694(03)00130-6

Marks, D., Winstral, A., Reba, M., Pomeroy, J., & Kumar, M. (2013). An evaluation of methods for determining during-storm precipitation phase and the rain/snow transition elevation at the surface in a mountain basin. *Advances in Water Resources*, *55*, 98–110. https://doi.org/10.1016/j.advwatres.2012.11.012

Maurer E and, Duffy PPB. 2005. Uncertainty in projections of streamflow changes due to climate change in California. *Geophysical Research Letters 32* (3): L03704. https://doi.org/10.1029/2004GL021462

Monteith, J. L. (1965). Evaporation and environment. *Symposia of the Society for Experimental Biology*, *19*, 205–234.

Nash, J. E., & Sutcliffe, J. V. (1970). River flow forecasting through conceptual models part I—A discussion of principles. *Journal of Hydrology*, *10*(3), 282–290. https://doi.org/10.1016/0022-1694(70)90255-6

Nolin, A. W., & Daly, C. (2006). Mapping 'at risk' snow in the Pacific Northwest. *Journal of Hydrometeorology*, *7*(5), 1164–1171. https://doi.org/10.1175/JHM543.1

Williams, A. P., Allen, C. D., Macalady, A. K., Griffin, D., Woodhouse, C. A., Meko, D. M., et al. (2012). Temperature as a potent driver of regional forest drought stress and tree mortality. *Nature Climate Change*, *3*(3), 292–297. https://doi.org/10.1038/nclimate1693

Peel, M. C., & Bloschl, G. (2011). Hydrological modelling in a changing world. *Progress in Physical Geography*, *35*(2), 249–261. https://doi.org/10.1177/0309133311402550

Philip, J. (1957). The theory of infiltration: 4. Sorptivity and algebraic infiltration equations. *Soil Science*, *84*, 257–263. https://doi.org/10.1097/00010694-195709000-00010

Richardson, J. J., Moskal, L. M., & Kim, S.-H. (2009). Modeling approaches to estimate effective leaf area index from aerial discrete-return LIDAR. *Agricultural and Forest Meteorology*, *149*, 1152–1160. https://doi.org/10.1016/j.agrformet.2009.02.007

Safeeq, M., Grant, G. E., Lewis, S. L., & Tague, C. L. (2013). Coupling snowpack and groundwater dynamics to interpret historical streamflow trends in the Western United States. *Hydrological Processes*, *27*(5), 655–668. https://doi.org/10.1002/hyp.9628

Son, K., Tague, C., & Hunsaker, C. (2016). Effects of model spatial resolution on ecohydrologic predictions and their sensitivity to inter-annual climate variability. *Water (Switzerland)*, *8*(8), 321. https://doi.org/10.3390/w8080321

Stephenson N, van Mantgem P. 2011. Causes and implications of the correlation between forest productivity and tree mortality rates. Ecological … 81 (4): 527–555 .https://doi.org/10.1890/10-1077.1

Tague, C., & Grant, G. E. (2009). Groundwater dynamics mediate low-flow response to global warming in snow-dominated alpine regions. *Water Resources Research*, *45*(7), W07421. https://doi.org/10.1029/2008WR007179

Tague, C., Heyn, K., & Christensen, L. (2009). Topographic controls on spatial patterns of conifer transpiration and net primary productivity under climate warming in mountain ecosystems. *Ecohydrology*, *2*(4), 541–554. https://doi.org/10.1002/eco.88

Tague, C., & Peng, H. (2013). The sensitivity of forest water use to the timing of precipitation and snowmelt recharge in the California Sierra: Implications for a warming climate. *Journal of Geophysical Research. Biogeosciences*, *118*(2), 875–887. https://doi.org/10.1002/jgrg.20073

Tague, C. L., & Band, L. E. (2004). RHESSys: Regional Hydro-Ecologic Simulation System—An object-oriented approach to spatially distributed modeling of carbon, water, and nutrient cycling. *Earth Interactions*, *8*(19), 1–42. https://doi.org/10.1175/1087-3562(2004)8<1:RRHSSO>2.0.CO;2

Teuling, A. J. (2005). Improved understanding of soil moisture variability dynamics. *Geophysical Research Letters*, *32*(5), L05404. https://doi.org/10.1029/2004GL021935

White, M. A., Thornton, P. E., Running, S. W., & Nemani, R. R. (2000). Parameterization and sensitivity analysis of the BIOME–BGC terrestrial ecosystem model: Net primary production controls. *Earth Interactions*, *4*(3), 1–85. https://doi.org/10.1175/1087-3562(2000)004<0003:PASAOT>2.0.CO;2

Zierl, B., Bugmann, H., & Tague, C. L. (2007). Water and carbon fluxes of European ecosystems: An evaluation of the ecohydrological model RHESSys. *Hydrological Processes*, *21*(24), 3328–3339. https://doi.org/10.1002/hyp.6540

SUPPORTING INFORMATION

Additional supporting information may be found online in the Supporting Information section at the end of the article.

How to cite this article: Son K, Tague C. Hydrologic responses to climate warming for a snow-dominated watershed and a transient snow watershed in the California Sierra. *Ecohydrology*. 2019;12:e2053. https://doi.org/10.1002/eco.2053